3198

Proceedings of the
Third International Symposium on

Refined Flow Modelling
and
Turbulence Measurements

26–28 July, 1988
Nippon Toshi Center
Tokyo

Edited
by
Y. IWASA
N. TAMAI
A. WADA

Scientific Organizing Committee of the Third International Symposium on Refined Flow Modelling and Turbulence Measurements

International Association for Hydraulic Research

Field Observation and Numerical Simulation of an Urban Wind

by
Dr. Jun-ichiro TSUTSUMI
JSPS Fellowships for Japanese Junior Scientists
Dept. of Thermal Energy System, Kyushu Univ.
6-1, Kasuga-koen, Kasuga-shi, Fukuoka 816, JAPAN

Dr. Tadahisa KATAYAMA
Professor
Dept. of Thermal Energy System, Kyushu Univ.
6-1, Kasuga-koen, Kasuga-shi, Fukuoka 816, JAPAN

Dr. Akio ISHII
Professor
Dept. of Environmental Design, Kyushu Institute of Design
9-1, Shiobaru 4 chome, Minami-ku, Fukuoka 815, JAPAN

Dr. Masaru NISHIDA
Professor
Dept. of Architecture, Kyushu Sangyo Univ.
327, Matsugadai 2 chome, higashi-ku, Fukuoka 813, JAPAN

SUMMARY

Wind speed and air temperature profiles are measured in an urbanized area. The two-dimensional space for numerical simulation of an urban wind is modelled after the field observation area. The Large Eddy Simulation (LES) is applied as a turbulence model. The effects of grid systems, turbulence conditions on the inflowing boundary and the Smagorinsky constant on the results of the numerical simulation are examined comparing with the results of the field observation.

1. Introduction

The urban wind is here defined as the wind which is blowing over an urban area. Urban atmospheric and thermal environment is greatly influenced by the urban wind(3). Especially, it is a well-known fact that the sea breeze relieves the urban thermal environment which grows worse in summer(1). In order to utilize the urban wind better it is necessary to grasp the characteristics of the urban wind in the actual condition and to predict it in the various planned cases. The urban wind is non-isotropic, non-isothermal turbulent air flow. Numerical simulation of turbulent air flow is expected to be the very method to predict the urban wind. However, the urban wind is a difficult object for numerical simulation because of its magnitude and boundary condition. It is too large to calculate in the inner layer, and not so large as the general circulation of atmosphere. The configuration and temperature distribution on the ground surface and the turbulent component of inflowing wind speed are very complicated.

The application of the Large Eddy Simulation (LES) to the prediction

of the urban wind is tried in this paper.. The urban area that is to be calculated is a simplified model based on the field observation, which is conducted in a seaside city. The objective wind for numerical simulation is the sea breeze. Several cases of numerical simulation are carried out and examined comparing with the field observation data.

2. Field Observation of an Urban Wind

2.1 Observation Points

The field observation of an urban wind is conducted in the Fukuoka city, Japan. Fukuoka is contiguous to the bay of Hakata by the northern border. The observation area is shown in Fig. 1. There are two parks, Nishi park and Ohori park, the rest of this area is almost covered with buildings. The ground surface of this area is nearly horizontal level except Nishi park which is a hill of 40m high. Ohori park has a large pond. Three points are fixed to measured the profiles of wind speed and air temperature. They are Point A, Point B and Point C, shown in Fig. 1. Point A is located on the seashore. Point B and Point C are located at the northern and the southern end of Ohori park. Ground and water surface temperature is measured at Point D and Point E, respectively. Point D is in a small park in the dwelling area. Point E is on an islet in the pond.

2.2 Observation Procedure

The profiles of wind speed and air temperature are measured at three points simultaneously by three tethersonde systems(5). The wind speed data are recorded in magnetic tapes, which is converted into digital data at intervals of 2 seconds. The measurement heights for the profiles are 5, 10, 15, 20, 25, 30, 35, 40, 50, 60 and 80m. These data are measured for 5 minutes at each height, and there are 1 minute intervals among them. Therefore, it takes 65 minutes for a series of the measurement. The wind speed data are non-dimensionalized by divided by reference wind speed, taking the long term fluctuation of wind speed into account. The reference wind speed is measured at a fixed height by 3-cup anemometers at each point, simultaneously. 12 series of the measurement are carried out at intervals of 2 hours all day long. The ground and water surface temperature are measured by infrared thermometers. Both the bare ground and the asphalt surface temperature are measured as the ground surface temperature.

2.3 Observation Results

The field observation term, 27-28 Aug., 1985, was fine, and the sea breeze blew clearly from 10 to 19 o'clock(5). The diurnal

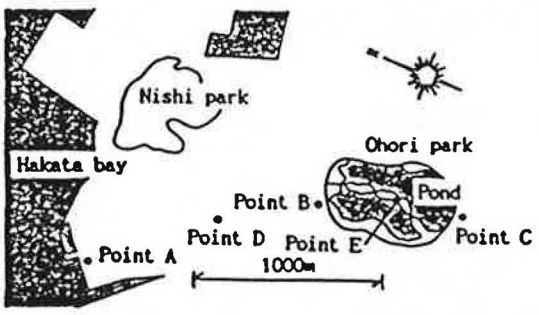

Fig. 1. Observation Points in Fukuoka city

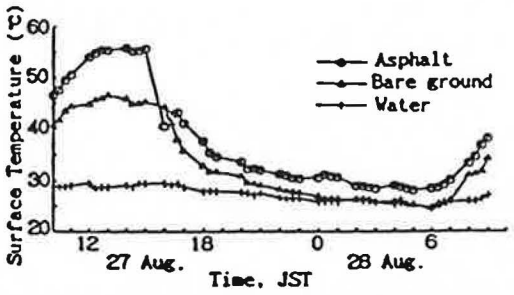

Fig. 2. Diurnal Fluctuation of Ground and Water Surface Temperature

fluctuations of three kinds of surface temperature are shown in Fig. 2. The water surface temperature is almost constantly 29℃ all day long, while the asphalt and the bare ground surface temperature range from 25 to 56℃ and from 28 to 47℃, respectively. The water surface temperature is regarded as the basis temperature, and the average of the asphalt and bare ground surface temperature is supposed to be the ground surface temperature. The difference between them is regarded as the representative temperature difference. These values are used to non-dimensionalize temperature data. The profiles of the non-dimension mean wind speed are shown in Fig. 3. These profiles are found in log-log scale from the average of the mean wind speed of the sea breeze. The profile of Point A is almost constant, and this wind speed is regarded as the representative velocity. The profiles of Point B and Point C are fit for the Power law with exponents of 1/4 and 1/8, respectively. The profiles of the average turbulence intensity of the sea breeze are shown in Fig. 4. Turbulence intensity at Point A is the smallest and almost 10% uniformly above the height of 20m, while it is larger in the lower part owing to the surface roughness. Turbulence intensity at Point B is larger in the lower part and smaller in the higher part than that at Point C. The profile of air temperature at Point A is shown in Fig. 5. These temperature data are non-dimension average values of the sea breeze hours. The air temperature at Point A means the sea breeze temperature. The average air temperature of the sea breeze is almost equal to the basis temperature above the height of 15m, while the air temperature in the lower part is influenced by the ground surface temperature.

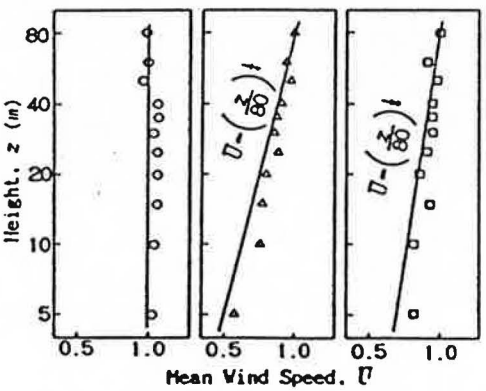

Fig. 3. Mean Wind Speed Profiles of the Sea Breeze in Log-Log Scale

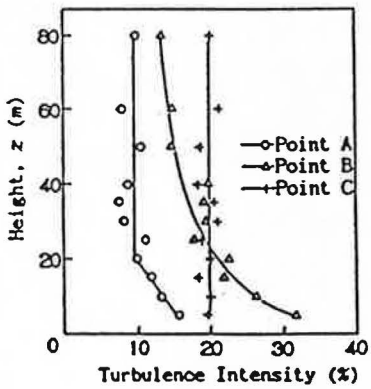

Fig. 4. Turbulence Intensity Profiles of the Sea Breeze

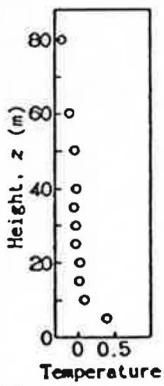

Fig. 5. Temperature profile at Point A

3. Numerical Simulation Space

The actual purpose of the numerical calculation carried out here is to simulate the measured sea breeze. The space for the numerical simulation has to be similar to the observation area. However, the configuration of the ground surface is so complicated, that it is almost impossible to model it entirely similarly. The measurement points are assumed in a line, that is the streamwise direction of the sea breeze. The air flow distribution in the spanwise direction is not considered in the field observation. Then, a two-dimensional rectangular space shown in Fig. 6. is fixed for the numerical simulation.

The streamwise and the vertical axis is x and z, respectively. The length in x direction is 2000m, that is nearly equal to the distance between Point A and Point C. Point B is 1200m leeward from Point A. The length in z direction is 80m, that is the height of the field observation. This height is regarded as the representative length to non-dimensionalize the length. Consequently, this area is the length of 25 and the height of 1 in the non-dimension scale.

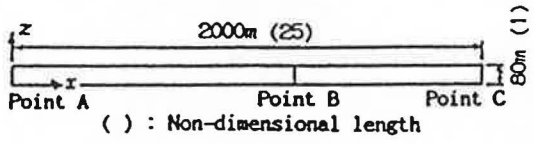

Fig. 6. Numerical Simulation Space

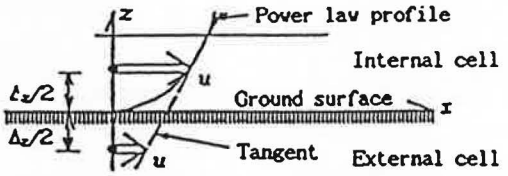

Fig. 7. Boundary Condition on the Ground Surface

4. Numerical Simulation of an Urban Wind

4.1 Governing Equations

The LES is adopted here as a turbulence model. The equation of continuity, the Navier-Stokes equations and the energy equation, the governing equations of air flow, are filtered using a top-hut filter function(2,6). The filtered equations are expressed as follows:

$$\frac{\partial u_i}{\partial x_i}=0 \tag{1}$$

$$\frac{\partial u_i}{\partial t}+\frac{\partial}{\partial x_j}(u_i u_j)=-\frac{\partial p}{\partial x_i}+\frac{\partial}{\partial x_j}\left(\nu_{SGS}\cdot e_{ij}+\frac{1}{Re}\frac{\partial u_i}{\partial x_j}\right)+\delta_{2i}\frac{Gr}{Re^2}\theta \tag{2}$$

$$\frac{\partial \theta}{\partial t}+\frac{\partial}{\partial x_i}(u_i\theta)=\frac{\partial}{\partial x_i}\left(\chi_{SGS}\frac{\partial \theta}{\partial x_i}+\frac{1}{Re\cdot Pr}\frac{\partial \theta}{\partial x_i}\right) \tag{3}$$

$$e_{ij}=\frac{\partial u_i}{\partial x_j}+\frac{\partial u_j}{\partial x_i} \tag{4}$$

where, u_i is the component of the velocity vector of the grid scale in the x_i direction, i=1 means x, i=2 means z, t is time, p is pressure with the subgrid scale (SGS) turbulence pressure, θ is temperature, ν_{SGS} is the SGS eddy viscosity, χ_{SGS} is the SGS eddy diffusion coefficient, δ_{ij} is the Kronecker's delta, Re is the Reynolds number, Gr is the Grashof number, Pr is the Prandtl number. Here, the Leonard stress terms and the cross terms in the Navier-Stokes equations and the terms in the energy equation which correspond to them are supposed to be ignored. Temperature is treated as a passive scalar without the buoyancy term. ν_{SGS} and χ_{SGS} are found by the Smagorinsky model(7) as follows:

$$\nu_{SGS}=(C_s\cdot\Delta)^2\cdot\left[\frac{(e_{ij})^2}{2}\right]^{\frac{1}{2}} \tag{5}$$

where, C_s is the Smagorinsky constant, Δ is the characteristic filter width. χ_{SGS} is here supposed to be equal to θ_{SGS}. This is rather simplified modelling for the non-isothermal turbulent air flow.

4.2 Calculation Procedure

The actual numerical simulation is carried out by the algorism of the MAC method on the staggered grid system(4). The spatial derivatives of all equations are approximated by centered differences, and forward differences are used for time integral.

Boundary conditions of the tangential velocity component on the ground surface including the water surface are defined as shown in Fig. 7. Namely, the velocity profile is assumed to be fit to the power law. The velocity in the external cell is found from the tangent of the power law profile, that is defined at the calculation point of the velocity in the internal cell. The exponents of the power law between Point A and Point B, Point B and Point C are assumed 1/4 and 1/8, respectively, from the results of the field observation. The normal velocity on the ground surface and on the upper limit is fixed 0. The free slip condition is adopted for the tangential velocity and the temperature on the upper limit and on the outflowing boundary. The normal velocity on the outflowing boundary is also free slip. The tangential velocity and the temperature on the inflowing boundary is fixed 0. The initial values of all variables are 0, except the normal velocity on the inflowing boundary and the ground surface temperature.

4.3 Cases of Numerical Simulation

As the instant values of the variables can be solved by the LES, the turbulent component of the velocity on the inflowing boundary should be examined. The streamwise and the vertical grid scale, those are Δ_x and Δ_z, and their ratio are very important factor in the LES, because the characteristic filter width, Δ, is decided from them. It is another problem how to decide Δ from Δ_x and Δ_z. Here, 15 cases of numerical simulation condition, shown in Table 1, are fixed, changing these factors and the Smagorinsky constant, C_s. The inflowing boundary

Table 1. Cases of Numerical Simulation

No.	Grid system (Δ_x , Δ_z)	Inflow Boundary	C_s	Δ
1	40x16 (0.6250,0.0625)	Constant	0.10	$(\Delta_x \cdot \Delta_z)^{\frac{1}{2}}$
2	40x16 (0.6250,0.0625)	Normal random	0.10	$(\Delta_x \cdot \Delta_z)^{\frac{1}{2}}$
3	40x16 (0.6250,0.0625)	Uniform random	0.10	$(\Delta_x \cdot \Delta_z)^{\frac{1}{2}}$
4	(40+40)x16 (0.6250,0.0625)	Approach flow	0.10	$(\Delta_x \cdot \Delta_z)^{\frac{1}{2}}$
5	40x16 (0.6250,0.0625)	Constant	0.12	$(\Delta_x \cdot \Delta_z)^{\frac{1}{2}}$
6	40x16 (0.6250,0.0625)	Constant	0.14	$(\Delta_x \cdot \Delta_z)^{\frac{1}{2}}$
7	40x16 (0.6250,0.0625)	Constant	0.17	$(\Delta_x \cdot \Delta_z)^{\frac{1}{2}}$
8	40x16 (0.6250,0.0625)	Constant	0.20	$(\Delta_x \cdot \Delta_z)^{\frac{1}{2}}$
9	80x16 (0.3125,0.0625)	Constant	0.10	$(\Delta_x \cdot \Delta_z)^{\frac{1}{2}}$
10	200x16 (0.1250,0.0625)	Constant	0.10	$(\Delta_x \cdot \Delta_z)^{\frac{1}{2}}$
11	400x16 (0.0625,0.0625)	Constant	0.10	$(\Delta_x \cdot \Delta_z)^{\frac{1}{2}}$
12	200x40 (0.1250,0.0250)	Constant	0.10	$(\Delta_x \cdot \Delta_z)^{\frac{1}{2}}$
13	400x80 (0.0625,0.0125)	Constant	0.10	$(\Delta_x \cdot \Delta_z)^{\frac{1}{2}}$
14	40x16 (0.6250,0.0625)	Constant	0.10	$(5\Delta_x \cdot \Delta_z)^{\frac{1}{2}}$
15	40x16 (0.6250,0.0625)	Constant	0.10	Δ_x

'Constant' means that the normal velocity on the inflowing boundary is constantly fixed 1, 'Normal random' and 'Uniform random' mean that the normal and uniform pseudorandom numbers are given to the velocity, their mean are 1 and their turbulence intensity are fit to the field observation. 'Approach flow' means that the extra space, which is correspond to the sea and has the same length as the original space, is attached windward. Non-dimensional parameters, *Re*, *Gr* and *Pr* are decided from the field observation, namely they are 0.5×10^{8}, 0.8×10^{15} and 0.7, respectively.

5. Numerical Simulation Results

All the results of the numerical simulation are examined comparing with the field data. As the values at Point A is the given condition, they are compared at Point B and Point C in relation to mean wind speed, turbulence intensity and mean temperature. The representative time of these numerical simulation is 10 seconds, supposing the representative wind speed is 8*m/s*. The non-dimension time 30 corresponds to 5 minutes, that is the measurement time of the field observation. All the numerical simulation results indicated here are found statistically from the data for 50-80 in the non-dimension time.

Comparison of the inflowing boundary conditions is shown in Fig. 8. There is not a great difference between them. The temperature profiles do not agree to the field data especially at Point B. It seems unnecessary to use the random number or approach flow calculation.

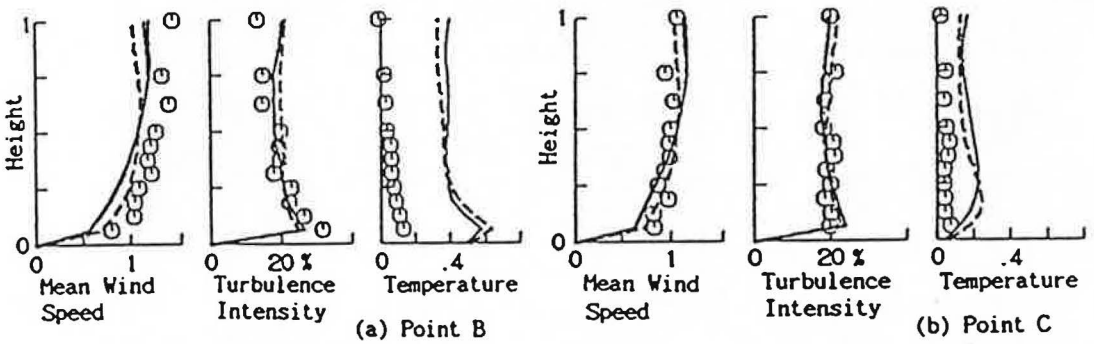

① : Field ——: No. 1 -----: No. 2 ——: No. 3 -----: No. 4

Fig. 8. Comparison of the Inflowing Boundary Conditions

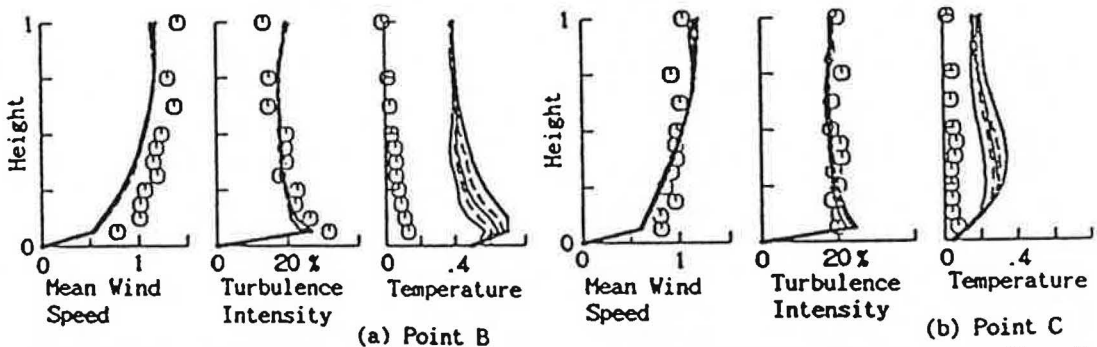

① : Field ——: No. 1 ----: No. 5 ——: No. 6 ----: No. 7 ——: No. 8

Fig. 9. Comparison of the Smagorinsky Constants

Comparison of C_s is shown in Fig. 9. They are almost the same values in relation to the mean wind speed and turbulence intensity. As to the temperature, the greater C_s is, the more distant from the field data. C_s=0.1 is thought to be the best of them. Comparison of the length and height ratios of grids is shown in Fig. 10. The ratio is changed by the length of a grid. When the grid length is shortened, the turbulence intensity grows larger and becomes distant from the field data, while the temperature is closer to the field data. Δ_z/Δ_x=1/5 seems the best results considering all the indicated data. Comparison of the grid size is shown in Fig. 11. Δ_z/Δ_x of these cases is fixed 1/5.

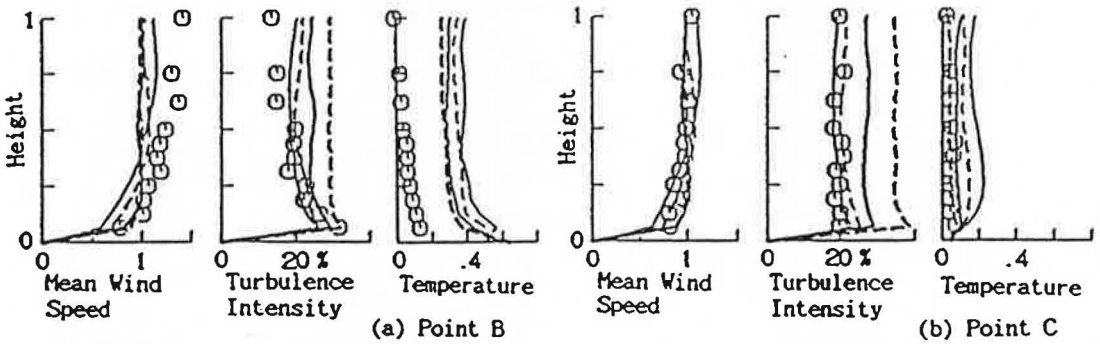

① : Field ——: No. 1 ----: No. 9 ——: No. 10 ----: No. 11

Fig. 10. Comparison of the Length and Height Ratios of Grids

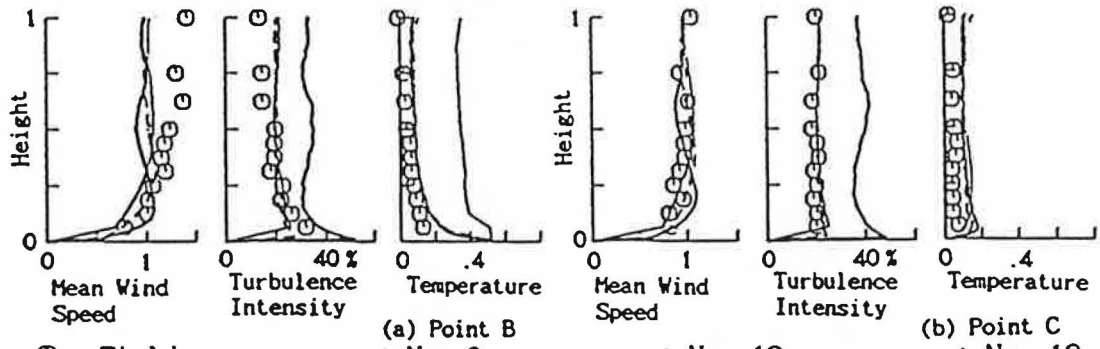

① : Field ——: No. 9 -----: No. 12 ——: No. 13

Fig. 11. Comparison of the Grid sizes in the Same Ratio

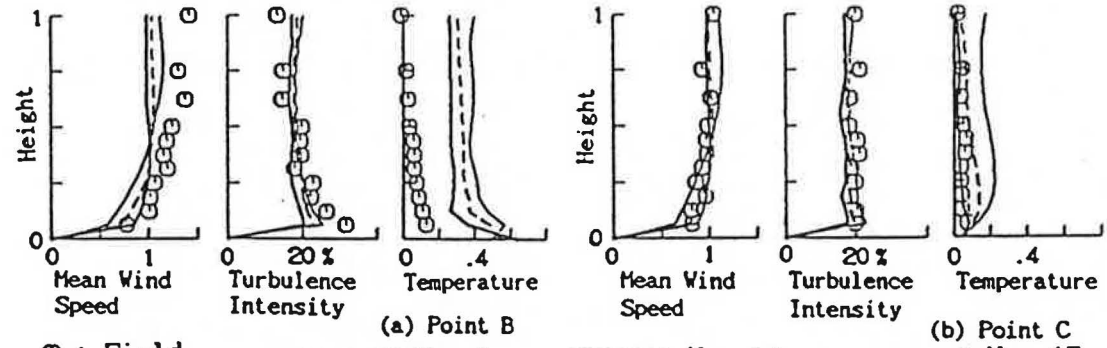

① : Field ——: No. 1 -----: No. 14 ——: No. 15

Fig. 12. Comparison of the Characteristic Filter Width

The turbulence intensity of the finest grid and the temperature of the most rough grid are too large. Both the turbulence intensity and the temperature of the middle size grid, No. 12, agree with the field data. These results make the necessity of the appropriate grid clear. As the grid scale has direct influence on Δ, three kinds of Δ on a grid are compared in Fig. 12. There is a little improvement in the temperature profile, when the definition of Δ is changed from the ordinary way. It is, however, not enough in relation to the temperature at Point B. The influence by the definition of Δ is much smaller than that by the grid size.

6. Conclusion

The sea-land breeze blowing over an urban area was two-dimensionally measured by tethersonde systems, and the sea breeze was numerically simulated using the simplified model based on the field observation by the LES. The results of several cases of the numerical simulation partially agree with the field observation data, however, it is difficult to fit them totally. There are some factors to be considered in the LES, the grid scale is the greatest factor that influences the results. However, it is not easy to decide the appropriate grid system, because these changeable factors have to be correlated one another. The boundary conditions in the numerical simulation model are designed after the field observation results. These conditions should be solved numerically in order to adapt numerical simulation to various cases without field data.

7. Reference

1. Asai, T. (1977), "Sea-Land Breeze", Scientific American Japan Edition, Extra No. 18, Nov., pp. 87-93. (in Japanese)

2. Deardorff, J. W. (1970), "A Numerical Study of Three-Dimensional Turbulent Channel Flow at Large Reynolds Number", J. of Fluid Mechanics, Vol. 41, Part 2, pp. 453-480.

3. Emonds, H. (1977), "Impacts on Urban Population from Climate and Immisions Caused by Buildings", Int. Conf. on Tall Buildings and Urban Habitat, Pre. Rep. Vol. II, Dec., pp. 77-85.

4. Harlow, F. H. and Welch, J. E. (1965), "Numerical Simulation of Time-Dependent Viscaus Incompressible Flow of Fluid with Free Surface", The Physics of Fluids, Vol. 8, No. 12, pp. 2182-2189.

5. Katayama, T., et al. (1987), "Observation of Heat Flux in an Urban Area with a Large Pond by Kytoons", Int. Conf. on Wind Eng., Priprint Vol. 1, July, pp.149-158.

6. Murakami, S., et al. (1987), "Three-Dimensional Numerical Simulation of Air Flow around a Cubic Model By Means of Large Eddy Simulation", J. of Wind Engineering and Industrial Aerodynamics, Mar., pp. 291-305.

7. Smagorinsky, J. S. (1963), "General Circulation Experiments with the Primitive Equations; Part 1", Monthly Weather Review, Vol. 91, pp. 99-164.